JAAS

Cite this: *J. Anal. At. Spectrom.*, 2011, **26**, 1502

www.rsc.org/jaas

PAPER

Elemental analysis of airborne particulate matter using an electrical low-pressure impactor and laser ablation/inductively coupled plasma mass spectrometry

Yi-Kong Hsieh,[a] Liang-Kai Chen,[a] Hui-Fang Hsieh,[a] Chih-Hung Huang[a] and Chu-Fang Wang*[ab]

Received 8th November 2010, Accepted 31st March 2011
DOI: 10.1039/c0ja00207k

In this study, we investigated the elemental contents of airborne particulate matter, having dimensions in the nanometer (<0.1 μm), submicrometer (0.1–1.0 μm), and micrometer (>1.0 μm) size ranges, collected using an electrical low-pressure impactor (ELPI). We used laser ablation/inductively coupled plasma mass spectrometry (LA-ICP-MS) to analyze the airborne particles trapped on filter media and to determine their elemental compositions. To simulate the ELPI collection of samples, we prepared laboratory-made standard filter samples by placing drops of liquid standard solutions onto the filter. The absolute limits of detection ranged from 2×10^{-2} ng for Cd to 1.06 ng for Si. The mean relative standard deviation for five replicates using the standard filter ranged from 3.5 to 17.8%. To determine the accuracy of this protocol, we analyzed the airborne particles using a standard addition method. Comparison with the data obtained using a dichotomous sampler/ICP-MS method revealed that our proposed ELPI/LA-ICP-MS method allowed the elemental and physical characteristics of ultra-fine particles in the atmosphere to be monitored with suitable accuracy to satisfy the needs of environmental, safety, and health applications.

1. Introduction

Airborne particles having diameters of 1 μm or less (PM_1) are considered to be potential threats to human health. Although abundant, these fine particles contribute little to the total mass of the material;[1] they have drawn the attention of researchers because of their high alveolar deposition fraction, large surface area, ability to induce inflammation, and potential to translate into the blood circulation system. In addition, exposure to low-solubility ultrafine (<100 nm) particles might cause more serious damage than exposure to larger particles;[2] some attempts have been made to link health effects or toxicity measurements with number concentration and chemical composition.[3–6] Hence, with our current high sampling and analytical abilities, there is increasing interest in studying particles having aerodynamic diameters of less than 0.1–1 μm.

Although the analysis of airborne particles in the submicrometer (<1 μm) regime is a challenging task, interest in the analysis of PM_1 or $PM_{0.1}$ is increasing.[7–19] In conventional airborne particle sampling and analysis, the sample is typically collected on a filter medium and dissolved in HNO_3 or in an HNO_3/HCl mixture for subsequent determination of its chemical components.[12,15] If the PM_{10} concentration were *ca.* 40 μg m^{-3}, 12 h of sampling using an air sampler operated at 10 L min^{-1} (typical for a commercial ultrafine particle sampler) would provide only 28.5 μg of collected submicrometer particles. Elements such as Fe, Ti, Cr, Zn, and Ba have been estimated to be present in such samples at contents in the range from 6 to 26%.[20] The levels of the toxic elements As, V, and Mn are commonly less than 0.1% in the collected samples. Therefore, many elements of interest are difficult to determine when using conventional analytical methods. It is common for the sampling period to be extended to reach the instrument's detection limits; as a result, we would expect poorly time-resolved analytical results. In addition, several other analytical problems have been encountered during airborne particle analyses, including difficulty weighing or digesting samples and the loss or contamination of trace elements in the course of the digestion process.

The direct analysis of solid samples has its advantage if the amount of sample is limited. Direct-filter analytical techniques or procedures involving little or no sample dissolution are becoming increasingly attractive because they do not require sample pretreatment and they reduce the degrees of sample contamination and loss and spectral interference. Several analytical methods, including instrumental neutron activation analysis,[7] proton-induced X-ray emission (PIXE),[8,14] X-ray fluorescence (XRF),[8,11–13,17–19] and laser ablation/inductively coupled plasma mass spectrometry (LA-ICP-MS),[16,21–25] have

[a]*Department of Biomedical Engineering and Environmental Sciences, National Tsing Hua University, Hsinchu, Taiwan. E-mail: cfwang@mx.nthu.edu.tw; Fax: +886-3-572-7298; Tel: +886-3-5715131 Ext.34222*
[b]*Institute of Nuclear Engineering and Science, National Tsing Hua University, Hsinchu, Taiwan*

been developed and applied to study the elemental compositions of airborne particulates. LA-ICP-MS is an analytical technology that has some of the advantages of ICP-MS (*e.g.*, very low detection limits for many elements, multi-element analysis capability, rapid scanning, and simple, easily interpreted spectra) while averting many of the problems associated with conventional airborne particle analysis using ICP-MS. There remains, however, a lack of a suitable standard material that covers the different needs of analyzing airborne particles by LA-ICP-MS. Strategies such as depositing a known amount of SRM 1648a on the filter[23,24] and elemental mapping of commercial SRM 2783 standard filters for calibration purposes[16] have been employed in the quantitative or semi-quantitative analysis of airborne particles by LA-ICP-MS. In addition, dried-droplet standards have been used for calibration in the analysis of drinking water and yeast.[29] Calibration with dried residues of standard solutions applied to a filter by micro-pipette has been used in the determination of airborne particles by LA-ICP-MS.[21,22] A similar method involving the use of pico-droplets generated by an inkjet printer has been proposed for the investigation of the elemental content of ultrafine particles by total reflection XRF (TXRF).[17]

The selection of the sampling device is a critical aspect when investigating airborne particles. In this study, we chose an electrical low-pressure impactor (ELPI), a type of cascade impactor for segregating dust into different particle sizes based on the principle of inertial impaction. Although the micro-orifice uniform deposit impactor (MOUDI) and other types of low pressure impactor have been used previously to collect PM_1 or $PM_{0.1}$ particles for subsequent ICP-MS and ICP-OES analysis,[9,10,26,27,33] the sample spots on the filter media collected using ELPI are better separated and more well-defined than those obtained using MOUDI. Simulating ELPI sample spots is possible by drying micro-droplet standard solutions onto the filter medium. The individual spots on both the sample and standard filter are suitable for LA-ICP-MS analysis; stoichiometric measurements can be achieved under appropriate ablation conditions.

In this study, we developed a strategy, combining ELPI with LA-ICP-MS, for the analysis of particulate matter. Droplets of standard solutions were dried on filter media used as standard filters. Although a similar method for calibrating LA-ICP-MS has been published, this study is the first to employ ELPI and LA-ICP-MS for the analysis of airborne particles having diameters of less than 1 μm.[21,22,28,29] To determine the absolute amounts of the elements in each standard and sample spot on the filter, it was necessary to ensure complete laser ablation through treatment of patterns of tiny spots on both of these filters. Calibration curves were obtained using a lab-made standard filter. For analytical accuracy, we used a standard addition method to verify the results of our proposed method and to evaluate the validity of this method of calibration. Furthermore, we also performed dichotomous sampling simultaneously with ELPI sampling, with analysis through acid-mixture digestion combined with liquid-introduction ICP-MS. Thereby, we compared the feasibility of using ELPI/LA-ICP-MS to analyze airborne particles in relation to the results obtained using the dichotomous sampler/ICP-MS.

2. Experimental

2.1 Collection of airborne particulate matter

Airborne particulates were collected in Hsinchu, Taiwan, in October 2008. An ELPI (Dekati) equipped with polytetrafluoroethylene (PTFE) membrane filters (Pall Zefluor, 25 mm diameter, 0.5 μm pore size) was used to collect airborne samples that had been segregated into different particle sizes. To investigate the elemental concentrations of nanometer (<0.1 μm), submicrometer (0.1–1.0 μm), micrometer (>1.0 μm), fine ($PM_{<2.5}$), and coarse ($PM_{2.5–10}$) airborne particles, aerosol samples were collected by the ELPI using two different combinations of sampling stages (Table 1). Three-stage (1, 3, and 8) ELPI aerosol samples were collected within a 4-h sampling period. The size ranges of the real filter samples were 0.030–0.108 μm for Sample A, 0.108–1.000 μm for Sample B, and 1.000–9.970 μm for Sample C. Two-stage ELPI (1 and 10) aerosol samples were also collected with 12-h sampling to compare the data with that from dichotomous sampling. The sampling flow rate was set at 10 L min^{-1} during the sampling period. Hydrophobic PTFE membrane filters were used in this study to collect the airborne particles because they allowed the ready preparation of lab-made standard filters through deposition of droplets of standard solutions.

The dichotomous sampler was operated at a total flow rate of 16.7 L min^{-1}. Two fractions, referred to as fine particles ($PM_{2.5}$) and course particles ($PM_{2.5–10}$), were collected on 37-mm Teflon membrane filters supported by polyolefin rings. All samples were collected during a 12-h sampling period for direct comparison with the data obtained through ELPI sampling.

Fig. 1 displays images of the airborne particles collected on the PTFE filters of stages (a) 1, (b) 3, (c) 8, and (d) 10 of the ELPI system. Marple *et al.* suggested that the ELPI substrates should be greased by painting heavy silicon oils onto the foils or filter media using a template prior to tare weighing.[30] Because this technique was highly likely to introduce chemical interference into our subsequent analyses, especially when determining Si, we did not use grease or silicon oil in this experiment. Fig. 1 also reveals that the sample spots on the filter medium collected by ELPI were separated and well defined. Therefore, we suspected that lab-made standard filters could be prepared to simulate real ELPI samples.

2.2 Preparation of standard filter

The limiting factor affecting quantitative analysis through LA-ICP-MS is the lack of suitable standards for calibration. In this study, we prepared solutions of the elements Na, Mg, Al, Si, K, Ca, Ti, V, Cr, Mn, Fe, Ni, Cu, Zn, As, Sr, Cd, Ba, and Pb by diluting 1000 mg L^{-1} single-element standard solutions used for ICP (Merck) with 2% Suprapur HNO_3 in purified water. We added methylene blue (*ca.* 250 ppm) to each prepared standard solution in order to locate the standard samples before and after laser ablation. Fig. 2(a) displays 0.5 μL drops of dyed standard solution that had been placed on a PTFE membrane filter using a micropipette. The droplet standard did not stick or permeate the hydrophobic filter surface. Fig. 2(b) reveals the absolute amounts of the target elements that had condensed on the filter after evaporation of the solvent. If the energy of the laser beam

Table 1 Collecting strategies and size distributions for the ELPI and dichotomous samplers

ELPI			Dichotomous sampler	
Size distribution (μm)	Filter types	Stage	*D*50% (μm)	Size distribution (μm)
1.000–9.970	C	13	9.97	
		12	6.8	2.500–10.00 ($PM_{2.5–10}$)
		11	4.4	
		10	2.5	
		9	1.6	
		8	1	
0.108–1.000	B	7	0.65	
		6	0.4	<2.500 ($PM_{2.5}$)
		5	0.26	
		4	0.17	
		3	0.108	
0.030–0.108	A	2	0.06	
		1	0.03	

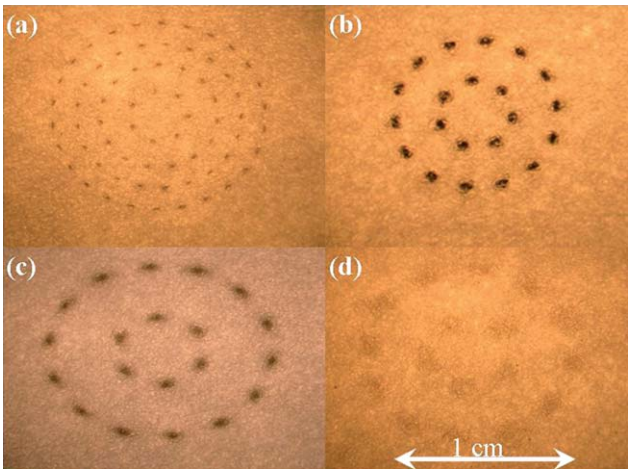

Fig. 1 Airborne particulates collected on the filters of the ELPI stages (a) 1, (b) 3, (c) 8, and (d) 10.

were sufficient to completely remove the airborne particulates (dried droplet standards) from the PTFE membrane filters, the integrated signal would represent the absolute amount of each sample (standard spot) and, thereby, allow quantitative analysis.

2.3 System configuration

Laser ablation was performed using a UP 213 laser ablation system (New Wave Research, USA) and a quadrupole ICP mass spectrometer (Agilent 7500a, USA). The laser beam (diameter: 110 μm; defocused distance: 1.5 mm) was used to vaporize the

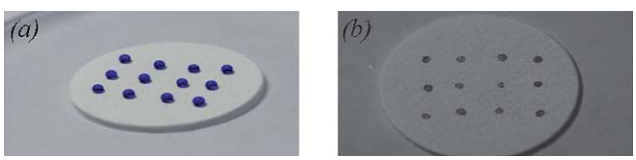

Fig. 2 Photographs of samples of a standard solution on the filter medium (a) before and (b) after evaporation of the solvent (water).

elements in a selected area of the collected airborne particle or dried-droplet standard spot without breaking the filter. Because the sizes of the sample spots were varied for the different collection stages, a 3 × 2 grid laser pattern (six shooting sites) was selected to ablate each impaction spot on the filters of samples A and B as well as on the standard filters, while a 3 × 3 grid laser pattern (nine shooting sites) was selected to ablate each impaction spot on the filters of the collection sample C. Detailed LA-ICP-MS operating parameters are given in Table 2.

2.4 Laser ablation

Fig. 3 demonstrates the procedure for the ablation of a single spot on sample C using a 3 × 3 grid laser pattern (nine shooting sites). The dotted circles represent the ablating areas using the proposed laser parameters, which formed a circle having a diameter of 500 μm. A 3 × 3 grid laser pattern having a 1000 μm × 1000 μm covering region was sufficient to ablate a spot on sample C. A 3 × 2 grid laser pattern covering a region of 1000 μm × 750 μm was suitable for ablating standard filters and samples A and B.

2.5 ELPI/LA-ICP-MS and dichotomous sampler/ICP-MS analyses

To verify the accuracy of the proposed method, the standard addition method was applied to the trace analysis of the multi-element laboratory standards. The standard concentration was adjusted appropriately for the sample and standard additions to

Table 2 Optimized operating conditions for LA-ICP-MS

Laser ablation (NewWave Research UP 213)	
Laser type	Nd : YAG
Laser mode	Q-switched (Pulsed)
Wavelength	213 nm
Pulse length	4 ns
Repetition rate	10 Hz
Dwell time	8 s
Intersite pause	1 s
Spot size	110 μm
Number of grid spots	6 (for standard filter and samples A and B), 9 (for sample C)
Output energy	100%
Fluence	15–20 J cm^{-2}
Raster spacing	300 μm
Grid spacing	300 μm
Defocused distance	1.5 mm
Carrier gas flow rate	1.0 L min^{-1}
ICP-MS (Agilent 7500a)	
RF power	1.5 kW
Acquisition mode	Time-resolved analysis
Acquisition time/mass	0.1 s
Acquisition time	68 s (for standard filter and samples A and B), 95 s (for sample C)
Plasma gas flow rate	15 L min^{-1}
Auxiliary gas flow rate	2.0 L min^{-1}
Carrier gas flow rate	1.05 L min^{-1}

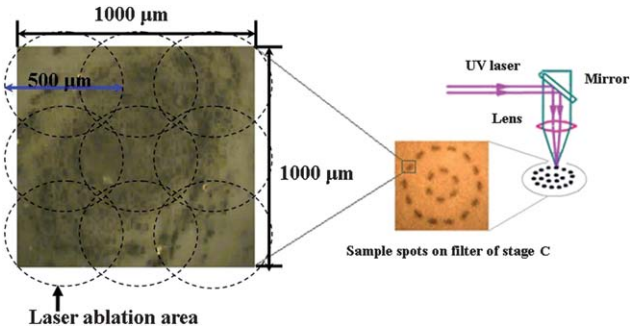

Fig. 3 Schematic representation of the laser grid pattern used to ablate a single spot on the filter of sample C.

be performed using 0.5 μL of the multi-element standard solution. The spiking levels were 0, 0.6, 1.2, 2.4, and 3 times the highest concentrations of the elements present in samples A, B, or C and each spiking level was randomly dropped on three sample spots. After spiking, the filter sample was placed in a drying cabinet to evaporate the solvent.

To evaluate the applicability of the proposed method, an $HNO_3/H_2O_2/HF$ (3 : 5 : 2, v/v/v) acid mixture and a previously described high-pressure bomb digestion method were employed to dissolve the samples collected in the dichotomous sampler.[31,32] NIST SRM1648(a) was conducted to ensure the precision of the digestion procedure. The spectrum mode in the Agilent 7500a ICP mass spectrometer was employed during these solution-based analyses.

3. Results and discussion

3.1 Laser ablation performance

Fig. 4 displays the qualitative scanning spectrograms of blank, standard, and real filter samples analyzed using LA-ICP-MS with a laser fluence of 16.7 J cm^{-2} and a defocused distance of 1.5 mm. The signals of many of the elements in the airborne particle samples were significantly higher than the background signals of the blank filter; calibration of these signals could be performed using the standard filter sample. For instance, the counts of ^{208}Pb obtained through LA-ICP-MS from the blank filter, standard filter, and samples A, B, and C were 100, 162 449, 5705, 105 266, and 79 064, respectively; the absolute amount of Pb on the standard filter was 5 ng. The calibration of these ^{208}Pb signals from real samples could, therefore, be conducted by using the signal of ^{208}Pb from the standard filter. The signals collected by the system could be integrated if the spots on both the standard filter and airborne particle samples could be ablated completely under the proposed operating conditions.

Fig. 5 illustrates the signal responses of ^{75}As toward the individual shots of a selected grid laser pattern onto the blank, real-sample, and standard-spot filters. Significant amounts of the standard and real samples were ablated during the first and second laser shots. We observe a general delay of the signal peak, which we attribute primarily to the time required to transport the sample from the laser ablation equipment to the ICP mass spectrometer. To ensure a comprehensive measurement, we employed total integrated times of 68 s for the standard filter and samples A and B and 95 s for sample C. The responses in Fig. 5

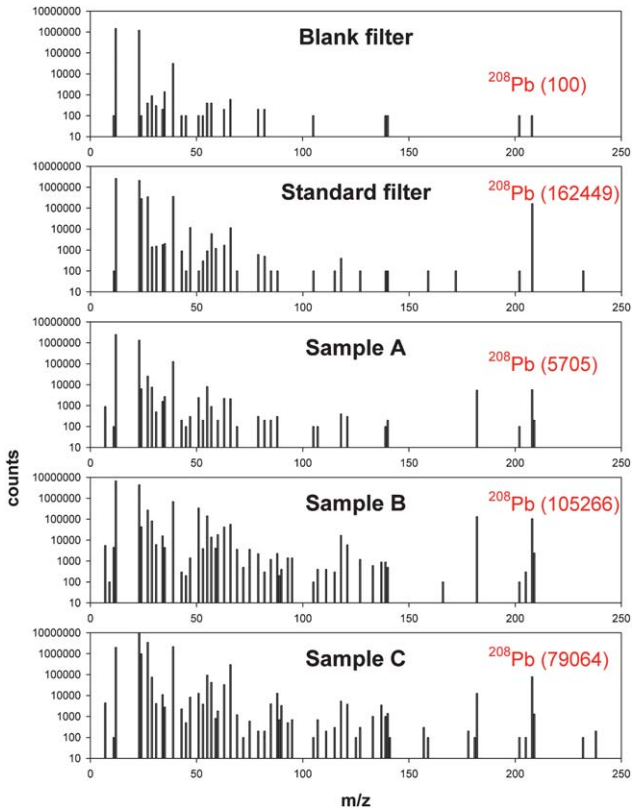

Fig. 4 Qualitative scanning spectrograms of the blank, standard, and real sample filters analyzed through LA-ICP-MS (operating conditions: laser fluence, 16.7 J cm^{-2}; defocused distance, 1.5 mm).

reveal that the laser could ablate the standard/sample spots entirely and that it was also possible to analyze ^{75}As quantitatively using the integration method. The integrated counts of each filter are indicated in parenthesis; the absolute amount of As on the standard filter was 1 ng. According to the data from the standard filter, approximately 0.15, 0.87, and 0.67 ng of As was present in each sample spot of samples A, B, and C, respectively.

To evaluate the extent of ablation, we re-scanned the same areas of the standard and sample filters. Fig. 6 displays the total

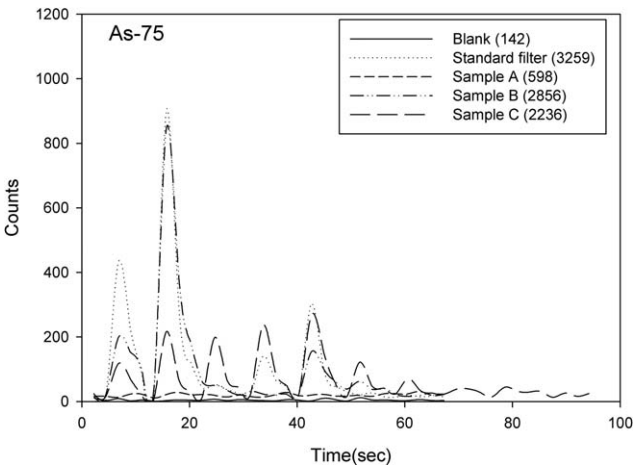

Fig. 5 Responses of ^{75}As ablated using the proposed laser grid patterns from the blank, standard, and real-sample filters.

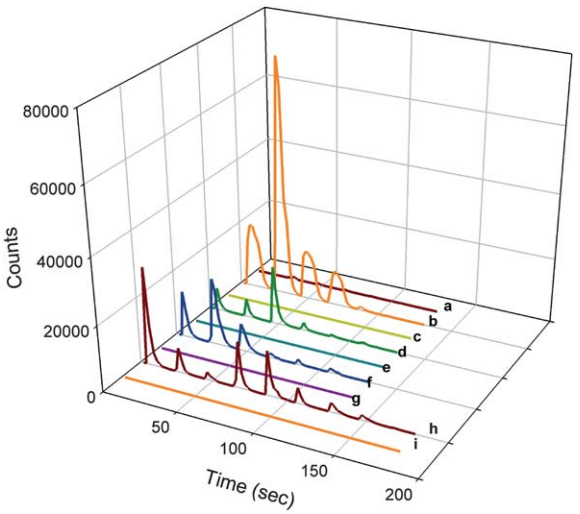

Fig. 6 Total analyte signals from the blank filter (a), standard filter (b, 1st scan; c, 2nd scan), and samples A (d, 1st scan; e, 2nd scan), B (f, 1st scan; g, 2nd scan), and C (h, 1st scan; i, 2nd scan).

analyte signals obtained through LA-ICP-MS from repetitive scans of the blank filter (a), the standard filter (b and c), and samples A (d and e), B (f and g), and C (h and i) Complete ablation occurred during the first scans (b, d, f, and h); the signals from the second scans (c, e, g, and i) were essentially equal to those from the blank filter (a). Thus, the energy of the laser beam was sufficient to remove the airborne particulates after the first ablation while maintaining the integrity of the filter substrates after the second.

3.2 Elemental determination by ELPI/LA-ICP-MS

For quantitative analysis, calibration curves are essential. Under the optimized conditions of LA-ICP-MS, we established calibration curves for all of the analyte elements from replicate analyses ($n = 5$) of laboratory-prepared standards of various loading on the PTFE-membrane filters. The measured intensities of each element generally increased upon increasing the concentration. Table 3 lists the correlation coefficients for the various analyte elements.

To determine the stability of the LA-ICP-MS analytical method, we measured its precision by repeatedly determining five different spots on a real sample (sample C). Table 4 reveals that the relative standard deviation (RSDs) for the analyte elements Na, Mg, Al, Ca, V, Cr, Mn, Fe, Cu, Zn, and As were less than 10%, while those for the other analytes (Si, K, Ti, Sr, Cd, Ba, Pb) were in the ranges from 10 to 15%. We attribute these fluctuations to heterogeneity among the sample spots collected by ELPI and also to the instability of the laser energy during the ablation process. Nevertheless, it is possible to randomly ablate five spots on a sample filter and reasonably estimate the concentrations of elements of interest from the obtained LA-ICP-MS data.

3.3 Validation of the proposed method

3.3.1 Standard addition. To validate the accuracy of our proposed method, we added standard solutions to the sample spots on the filter and then performed quantitative analysis using external standard calibration, as described above. After quantitative analysis, we applied the standard addition method to the rest of the sample spots on the same sample filter. For example, among the 20 impaction spots of sample C, we added standard solutions of different concentrations to the analytes on the 15 spots remaining on the filter after quantitative analysis. We determined the concentrations of the trace elements from the calibration curve, which was obtained based on the standard addition samples that had been ablated using the same laser ablation approach. Fig. 7 presents the standard addition curves for As on the various samples; they were obtained through linear least-squares regression of the integrated ion signal (y) versus the

Table 3 Detection limits (3σ) for all analyte elements and correlation coefficients (r^2) for the standard curves

Element	Slope ($\times 10^4$)	Intercept ($\times 10^3$)	Corr. coeff. (r^2)	LOD (ng)
^{23}Na	100	622	0.9751	0.173
^{24}Mg	36.4	70.2	0.9913	0.126
^{27}Al	23.6	142	0.9967	0.195
^{28}Si	7.42	199	0.9778	1.062
^{39}K	33.0	6.91	0.9837	0.079
^{43}Ca	0.05	0.87	0.9955	0.256
^{47}Ti	5.54	0.25	0.9976	0.007
^{51}V	60.9	0.65	0.9904	0.008
^{53}Cr	12.9	1.12	0.9712	0.011
^{55}Mn	73.6	8.71	0.9903	0.003
^{57}Fe	48.8	30.9	0.9950	0.157
^{60}Ni	7.06	0.02	0.9937	0.007
^{63}Cu	19.1	1.05	0.9935	0.009
^{66}Zn	1.68	0.59	0.9834	0.061
^{75}As	2.96	0.02	0.9847	0.003
^{88}Sr	17.4	0.68	0.9812	0.004
^{111}Cd	0.72	0.01	0.9929	0.002
^{137}Ba	1.37	0.02	0.9972	0.012
^{208}Pb	35.3	23.6	0.9903	0.083

Table 4 RSDs ($n = 5$) and mean signal counts obtained through LA-ICP-MS for the blank, laboratory-prepared standard, and real sample (sample C) filters

	Blank filter		Standard filter		Real sample	
Element	Counts	RSD (%)	Counts	RSD (%)	Counts	RSD (%)
^{23}Na	5 927 827	5.6	20 250 000	6.9	12 000 000	4.6
^{24}Mg	2065	14.7	13 125 000	10.4	248 322	1.2
^{27}Al	4641	8.7	51 525 000	10.3	657 016	4.2
^{28}Si	203 759	3.9	5 785 472	17.8	1 082 554	12.2
^{39}K	239 395	16.1	6 959 693	7.4	1 410 217	13.7
^{43}Ca	922	17.0	33 870	9.5	1222	4.0
^{47}Ti	189	8.1	55 984	3.5	5349	14.4
^{51}V	404	13.9	29 580	8.1	27 062	6.5
^{53}Cr	1086	13.9	16 410	17.1	4613	7.9
^{55}Mn	4457	13.2	248 069	11.5	216 047	9.6
^{57}Fe	2163	6.8	165 667	12.9	46 685	7.1
^{60}Ni	1104	6.1	5828	15.6	5645	7.9
^{63}Cu	5292	4.2	49 535	8.6	42 643	9.4
^{66}Zn	354	8.7	139 325	11.8	108 238	8.6
^{75}As	558	3.4	3416	9.1	2033	6.5
^{88}Sr	223	6.9	54 769	11.0	13 712	10.7
^{111}Cd	33	14.3	246	16.1	186	14.6
^{137}Ba	36	16.3	8726	15.5	3987	12.1
^{208}Pb	139	7.5	163 725	9.6	113 705	14.3

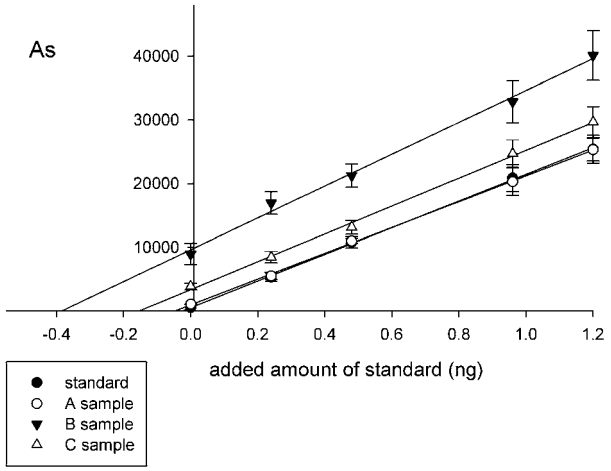

Fig. 7 Standard addition calibration curves for As in the sample spots on the standard filter and the real-sample filters A, B, and C.

amount of added analyte (x). The curve for sample A overlaps with that of the dried droplet liquid standard because of the negligible amount of As in sample A. For samples B and C, the As contents, obtained using the standard addition method, were 0.38 and 0.16 ng, respectively.

Table 5 compares the elemental contents of samples B and C obtained using the external standard calibration and standard addition calibration methods. The quantification of the elements V, Cr, Mn, Fe, Ni, Zn, As, and Pb in sample B and Na, Mg, Al, Ca, Mn, Fe, Ni, and Zn in sample C using dried-droplet liquid standard with both external standard calibration and standard addition are in agreement. For some elements, namely Mg, Al, K, and Cu in sample B and Si, K, Ti, Sr, and Pb in sample C, the results are significantly different, possibly because of the heterogeneity of the samples collected by ELPI. In other studies, the same phenomena was observed for bulk particles in airborne samples.[16,25] The coarse particles originating from rock and soil might change the signal obtained both from external standard calibration and standard addition.

Table 5 Elemental contents (ng) obtained from samples B and C using external standard calibration (ESC) and standard addition (SA)[a]

	Sample B		Sample C	
Element	ESC	SA	ESC	SA
Na	2.9	3.6	6.8	7.8
Mg	0.63	0.053	5.7	6.8
Al	0.88	4.4	19	17
Si	11	—	28	48
K	5.4	43	9.6	18
Ca	—	—	6.5	5.9
Ti	0.026	—	0.33	0.67
V	0.18	0.18	0.028	0.021
Cr	0.11	0.092	0.047	0.032
Mn	0.35	0.31	0.45	0.47
Fe	2.9	3.3	12	14
Ni	0.13	0.15	0.052	0.064
Cu	0.31	0.88	0.21	0.16
Zn	3.2	2.6	2.6	2.5
As	0.47	0.38	0.11	0.16
Sr	0.021	—	0.20	0.043
Cd	0.12	0.074	0.043	0.056
Ba	0.19	—	0.70	0.55
Pb	2.6	2.4	0.92	1.6

[a] —: Less than the detection limit.

3.3.2 Comparison of ELPI/LA-ICP-MS and dichotomous sampler/ICP-MS methods. To confirm the applicability of our proposed ELPI/LA-ICP-MS method for studying air pollution, we compared the experimental data obtained using ELPI/LA-ICP-MS and dichotomous sampler/ICP-MS after simultaneously collecting samples from the sampling site. When using ELPI, the $PM_{2.5}$ data were obtained in the first stage and the PM_{10} data were obtained by summing data from the first and tenth stages. We calculated the total elemental amount at each stage by multiplying the average absolute elemental mass loading per spot with the orifice number for the respective impaction plates. For example, the calculated total amount of As at the first stage would be 10.35 ng if the average absolute As mass loading per spot was 0.15 ng. The sum of the total elemental amount on different plates was divided by the volume of air (m^3) sampled on purpose to compare with the data obtained from the dichotomous sampler/ICP-MS (in ng m^{-3}). Fig. 8 displays the correlation between the PM_{10} and $PM_{2.5}$ data obtained using the dichotomous sampler and ELPI for Zn, Pb, and Cd in an aerosol sample collected in the Hsinchu area. The regression lines are forced through zero; the slope and correlation coefficient are provided for each element. The correlations of the various elements ranged from 0.6853 for Zn in PM_{10} to 0.8916 for Zn in $PM_{2.5}$. Overall, the two methods exhibited similar trends. Despite the lower degrees of contamination and chemical loss provided by LA-ICP-MS, several problems remained for our proposed method, including the instability of the laser beam energy and the high fluctuation in elemental concentrations

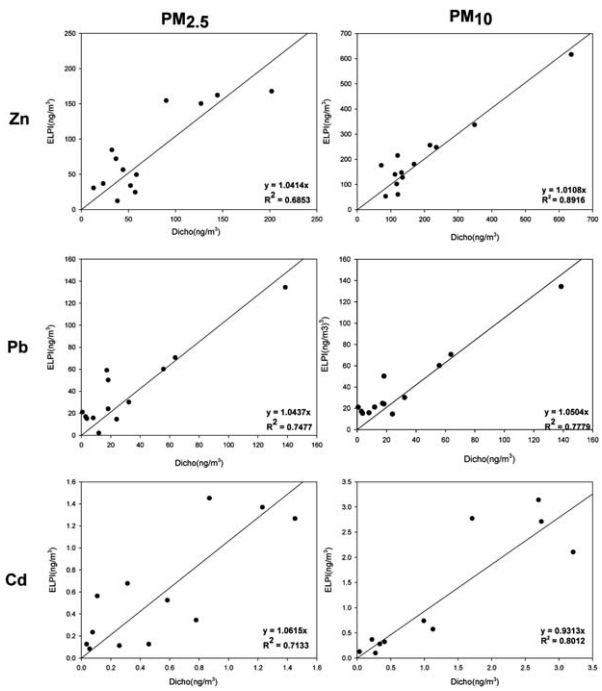

Fig. 8 Correlation between the PM_{10} and $PM_{2.5}$ data obtained using a dichotomous sampler (Dicho) and ELPI for Zn, Pb, and Cd in an aerosol sample collected in the Hsinshu area ($n = 13$).

caused by the heterogeneity of the samples collected by ELPI. On the other hand, the dichotomous sampler/ICP-MS method also suffers from problems, such as incomplete digestion, the loss or contamination of trace elements during the digestion process, and serious spectrometric interference resulting from acid-derived background ions during ICP-MS.

Conclusions

ELPI/LA-ICP-MS allows the simple and rapid quantitative analysis of the elemental components of nanometer- and sub-micrometer-sized airborne particles. Using this approach, we determined a total of 19 elements (Na, Mg, Al, Si, K, Ca, Ti, V, Cr, Mn, Fe, Ni, Cu, Zn, As, Sr, Cd, Ba, Pb) present in airborne particulate matter. This method has better detection limits and requires less sampling/analyzing time relative to that of other established protocols. Four hours of sampling was sufficient for the analysis of nanometer-, submicrometer-, and micrometer-sized airborne particulate matter; therefore, this approach offers improved time resolution for air pollution studies.

Acknowledgements

We thank the National Science Council, Taiwan for funding this project under contract number NSC99-2113-M-007-017 and the Instrument Center at National Tsing Hua University in Taiwan for the ICP-MS support.

References

1 P. Penttinen, K. L. Timonen, P. Tiittanen, A. Mirme, J. Ruuskanen and J. Pekkanen, *Eur. Respir. J.*, 2001, **17**, 428–435.
2 M. Jamriska, L. Morawska and D. S. Ensor, *Indoor Air*, 2003, **13**, 96–105.
3 R. D. Brook, B. Franklin, W. Cascio, Y. Hong, G. Howard, M. Lipsett, R. Luepker, M. Mittleman, J. Samet, S. C. Smith, Jr. and I. Tager, *Circulation*, 2004, **109**, 2655–2671.
4 A. Seaton, W. MacNee, K. Donaldson and D. Godden, *Lancet*, 1995, **345**, 176–178.
5 G. Oberdorster, E. Oberdorster and J. Oberdorster, *Environ. Health Perspect.*, 2005, **113**, 823–839.
6 J. S. Brown, K. L. Zeman and W. D. Bennett, *Am. J. Respir. Crit. Care Med.*, 2002, **166**, 1240–1247.
7 G. R. Cass, L. A. Hughes, P. Bhave, M. J. Kleeman, J. O. Allen and L. G. Salmon, *Philos. Trans. R. Soc. London, Ser. A*, 2000, **358**, 2581–2592.
8 A. Chung, J. D. Herner and M. J. Kleeman, *Environ. Sci. Technol.*, 2001, **35**, 2184–2190.
9 C. C. Lin, S. J. Chen, K. L. Huang, W. I. Hwang, G. P. Chang-Chien and W. Y. Lin, *Environ. Sci. Technol.*, 2005, **39**, 8113–8122.
10 G. C. Fang, Y. S. Wu, C. C. Wen, C. K. Lin, S. H. Huang, J. Y. Rau and C. P. Lin, *Toxicol. Ind. Health*, 2005, **21**, 259–271.
11 M.-C. Oliver Chang, J. C. Chow, J. G. Watson, C. Glowacki, S. A. Sheya and A. Prabhu, *Aerosol Sci. Technol.*, 2005, **39**(10), 947–959.
12 J. D. Herner, P. G. Green and M. J. Kleeman, *Environ. Sci. Technol.*, 2006, **40**, 1925–1933.
13 L. Ntziachristos, J. R. Froines, A. Cho and C. Sioutas, *Part. Fibre Toxicol.*, 2007, **4**, 5.
14 R. Miranda and E. Tomaz, *Atmos. Res.*, 2008, **87**, 147–157.
15 E. R. McKenzie, C. M. Wong, P. G. Green, M. Kayhanian and T. M. Young, *Sci. Total Environ.*, 2008, **398**, 145–153.
16 S. Gligorovski, J. T. V. Elteren and I. Grgic, *Sci. Total Environ.*, 2008, **407**, 594–602.
17 U. E. A. Fittschen, S. Hauschild, M. A. Amberger, G. Lammel, C. Streli, S. Förster, P. Wobrauschek, C. Jokubonis, G. Pepponi, G. Falkenberg and J. A. C. Broekaert, *Spectrochim. Acta, Part B*, 2006, **61**, 1098–1104.
18 A. Wagner, J. Boman and M. J. Gatari, *Spectrochim. Acta, Part B*, 2008, **63**, 1426–1431.
19 A. Wagner and M. Mages, *Spectrochim. Acta, Part B*, 2010, **65**, 471–477.
20 L. S. Hughes, G. R. Cass, J. Gone, M. Ames and I. Olmez, *Environ. Sci. Technol.*, 1998, **32**, 1153–1161.
21 S. Tanaka, N. Yasushi, N. Sato, T. Fukasawa, S. J. Santosa, K. Yamanaka and T. Ootoshi, *J. Anal. At. Spectrom.*, 1998, **13**, 135–140.
22 T. Okuda, J. Kato, J. Mori, M. Tenmoku, Y. Suda, S. Tanaka, K. B. He, Y. L. Ma, F. Yang, X. C. Yu, F. K. Duan and Y. Lei, *Sci. Total Environ.*, 2004, **330**, 145–158.
23 C. F. Wang, S. L. Jeng, C. C. Lin and P. C. Chiang, *Anal. Chim. Acta*, 1998, **368**, 11–19.
24 C. J. Chin, C. F. Wang and S. L. Jeng, *J. Anal. At. Spectrom.*, 1999, **14**, 663–668.
25 S. Rauch, M. Lu and G. M. Morrison, *Environ. Sci. Technol.*, 2001, **35**, 595–599.
26 N. J. Pekney, C. I. Dacidson, K. J. Bein, A. S. Wexler and M. V. Johnston, *Atmos. Environ.*, 2006, **40**, 411–S423.
27 L. Ntziachristos, Z. Ning, M. D. Geller, R. J. Sheesley, J. J. Schauer and C. Sioutas, *Atmos. Environ.*, 2007, **41**, 5684–5696.
28 U. E. A. Fittschen, N. H. Bings, S. Hauschild, S. Förster, A. F. Kiera, E. Karavani, A. Frömsdorf and J. Thiele, *Anal. Chem.*, 2008, **80**, 1967–1977.
29 L. Yang, R. E. Sturgeon and Z. Mester, *Anal. Chem.*, 2005, **77**, 2971–2977.
30 V. A. Marple, K. L. Rubow and S. M. Behn, *Aerosol Sci. Technol.*, 1991, **14**, 434–446.
31 C. F. Wang, C. Y. Chang, C. J. Chin and L. C. Men, *Anal. Chim. Acta*, 1999, **392**, 299–306.
32 C. Y. Chang, C. F. Wang, D. T. Mui and H. L. Chiang, *J. Hazard. Mater.*, 2009, **163**, 578–587.
33 A. Robache, F. Mathé, J. C. Galloo and R. Guillermo, *Analyst*, 2000, **125**, 1855–1859.

